Atherosclerosis 252 (2016) 166–174

Contents lists available at ScienceDirect

Atherosclerosis

journal homepage: www.elsevier.com/locate/atherosclerosis

NecroX-7 reduces necrotic core formation in atherosclerotic plaques of *Apoe* knockout mice

Mandy O.J. Grootaert [a, *], Dorien M. Schrijvers [a], Hanne Van Spaendonk [a], Annelies Breynaert [b], Nina Hermans [b], Viviane O. Van Hoof [c], Nozomi Takahashi [d, e], Peter Vandenabeele [d, e], Soon Ha Kim [f], Guido R.Y. De Meyer [a], Wim Martinet [a]

[a] Laboratory of Physiopharmacology, University of Antwerp, Antwerp, Belgium
[b] NatuRA, Laboratory of Nutrition and Functional Food Science, University of Antwerp, Antwerp, Belgium
[c] Department of Clinical Chemistry, Antwerp University Hospital, Antwerp, Belgium
[d] Inflammation Research Center, VIB, Ghent, Belgium
[e] Department of Biomedical Molecular Biology, UGent, Ghent, Belgium
[f] R&D Park, LG Life Sciences, Ltd., Daejeon, South Korea

ARTICLE INFO

Article history:
Received 24 December 2015
Received in revised form
10 June 2016
Accepted 29 June 2016
Available online 2 July 2016

Keywords:
Atherosclerosis
Inflammation
Mitochondrial ROS
Necrosis
NecroX-7

ABSTRACT

Background and aims: A large necrotic core is a key feature of atherosclerotic plaque instability. Necrotic cellular debris accumulates in the lipid-rich core and promotes inflammation, destabilization and ultimately rupture of the plaque. Although the role of necrosis in atherosclerosis is rather clear-cut, not many strategies have been performed up till now to specifically target plaque necrosis. In the present study, we tested the plaque stabilizing potential of NecroX-7, a novel compound with antioxidative and anti-necrotic properties.

Methods: Male apolipoprotein E (*Apoe*) knockout mice were treated with NecroX-7 (30 mg/kg) or vehicle, 3 times per week, via intraperitoneal injections for 16 weeks. Meanwhile, mice were fed a western-type diet to induce plaque formation.

Results: NecroX-7 reduced total plaque burden in the thoracic aorta as compared to vehicle-treated mice, without affecting total plasma cholesterol. Plaques in the aortic root of NecroX-7-treated mice showed a significant decrease in necrotic core area, 8-oxodG, iNOS and MMP13 expression, while collagen content and minimum fibrous cap thickness were increased. Moreover, NecroX-7 treatment reduced the expression of multiple inflammation markers such as *TNFα*, *IL1β*, *iNOS*, *HMGB1* and *RAGE* in a NF-κB-dependent manner. *In vitro*, NecroX-7 prevented *tert*-butyl hydroperoxide (tBHP)-induced mitochondrial ROS formation, necrosis, iNOS expression and HMGB1 release in primary macrophages.

Conclusions: NecroX-7 improves features of plaque stability in *Apoe* knockout mice by reducing necrotic core formation, oxidative stress and inflammation, and by increasing collagen deposition and fibrous cap thickness. Therefore, NecroX-7 could be a promising pleiotropic drug for the treatment of atherosclerosis.

1. Introduction

Formation and enlargement of a necrotic core plays a key role in the pathology of unstable atherosclerotic plaques [1]. In a detailed morphometric analysis of advanced human lesions, 80% of necrotic cores appeared to be larger than 1 mm^2 and comprised >10% of the plaque area [2]. However, in two thirds of the examined ruptured plaques, the necrotic core occupied >25% of the plaque [2]. Cellular debris of necrotic cells as well as the accumulation of lipids, most likely released by necrotic foam cells, contributes to necrotic core formation [3]. Necrotic cell death is morphologically distinguishable from other forms of cell death (e.g. apoptosis) by a gain in cell volume (oncosis) and swelling of organelles, followed by rupture of the plasma membrane and release of intracellular content [4]. The necrotic debris is a major source of damage-associated molecular patterns (e.g. high mobility group box 1 [HMGB1]), pro-inflammatory cytokines (e.g. IL6), proteases (e.g. matrix metalloproteinases [MMPs]) and pro-thrombotic factors (e.g. tissue

* Corresponding author. Laboratory of Physiopharmacology, University of Antwerp, Universiteitsplein 1B-2610, Antwerp, Belgium.
E-mail address: mandy.grootaert@uantwerpen.be (M.O.J. Grootaert).

http://dx.doi.org/10.1016/j.atherosclerosis.2016.06.045
0021-9150/

factor) [5] and thus can jeopardize plaque stability by promoting inflammation, plaque rupture (e.g. by thinning of the fibrous cap) and subsequent thrombosis [2]. Necrosis in atherosclerotic plaques is triggered by various stimuli including high levels of reactive oxygen species (ROS), ATP depletion and elevated intracellular calcium levels [6]. Moreover, impaired phagocytic clearance of apoptotic cells promotes secondary necrosis and expansion of the necrotic core [5,7]. Only since the late 1990's, the first conclusive evidence for necrotic cell death in human plaques was published [8,9]. Histological analysis of advanced lesions showed that the necrotic core is surrounded by dying macrophages and contains predominantly macrophage debris [3,8].

Despite the importance and potential therapeutic relevance of necrosis in human atherosclerosis, plaque necrosis has not been a subject of interest for many years. Possible reasons are the lack of reliable markers to detect necrosis and the poor availability of therapeutic agents to specifically target necrosis. Essentially, necrosis has long been considered as an accidental and uncontrolled form of cell death. However, this concept changed when researchers identified receptor-interacting protein (RIP) kinases, in particular RIPK1 and RIPK3, as key regulators in mediating programmed necrosis (also called necroptosis) [10–12]. *Ripk3*-deficient low density lipoprotein receptor (*Ldlr*) knockout mice show a significant reduction in the size of advanced plaques due to inhibition of macrophage necrosis [13], while early lesions are not affected. This finding suggests that RIPK3-mediated necroptosis promotes plaque instability in advanced plaques, but does not play a role in early plaque development.

Given that necrosis is a poorly investigated yet crucial phenomenon in atherosclerosis, we aimed to inhibit necrosis by targeting one of its main inducers, namely mitochondrial ROS. Numerous studies have demonstrated the importance of mitochondrial ROS in the progression of atherosclerosis both in patients and animal models [14–18]. High levels of ROS may lead to necrosis by causing irreversible damage of vital cellular components such as DNA, proteins and lipids. Recently, several research groups reported promising results after administration of NecroX compounds, a novel class of small molecules that exhibit antioxidative properties through ROS and RNS scavenging [19], NADPH oxidase inhibition [20] and inhibition of mitochondrial ROS generation [21]. Moreover, NecroX compounds have been shown to prevent oxidative-stress induced necrotic cell death [19,20], to inhibit HMGB1-mediated inflammatory responses [22] and to protect against myocardial necrosis after ischemia-reperfusion injury [23]. Furthermore, NecroX-7 is currently being tested in ST-segment elevated myocardial infarction (STEMI) patients undergoing percutaneous coronary intervention (https://clinicaltrials.gov, identifier NCT02070471). Based on these findings, we were encouraged to evaluate the potential plaque stabilizing effects of NecroX-7 in atherosclerosis. Our data indicate that NecroX-7 increases features of plaque stability in western-type diet fed apolipoprotein E knockout (*Apoe*$^{-/-}$) mice by reducing necrotic core formation, suppressing oxidative stress, lowering plaque inflammation and increasing collagen deposition and fibrous cap thickness.

2. Materials and methods

2.1. Mice

Male *Apoe*$^{-/-}$ mice (C57BL/6, Jackson Laboratory, stock number 002052) were fed a western-type diet (4021.90, AB Diets) for 16 weeks. Simultaneously, mice were treated with NecroX-7 (LG Life Sciences, 30 mg/kg body weight) (n = 25) or vehicle (water for injection) (n = 26) via intraperitoneal injections 3 times per week. Mice were housed in a temperature-controlled room with a 12 h light/dark cycle and food and water *ad libitum*. At the end of the experiment, mice were fasted overnight and blood was collected by cardiac puncture. Total cholesterol, LDL cholesterol and triglyceride levels were measured on a Dimension Vista® System (Siemens Healthcare Diagnostics) with reagents from the same manufacturer. Plasma levels of oxLDL and malondialdehyde (MDA) were measured by an ELISA (USCNK, SEA527Mu) and a HPLC-fluorescence detection method [24], respectively. Tissues were imbedded in Neg-50 Frozen Section Medium and stored at −80 °C or fixed in formalin 4% for 24 h before paraffin imbedding. For *in vitro* experiments, wild-type mice (C57BL/6, Jackson Laboratory, stock number, 000664) and *Ripk3*$^{-/-}$ mice were used. *Ripk3*$^{-/-}$ mice, produced by targeted gene deletion [25], were a generous gift from K. Newton and V. Dixit (Genentech, San Francisco). All experiments were approved by the Ethical Committee of the University of Antwerp.

2.2. Histological analysis

The thoracic aorta was stained *en face* with Oil Red O (ORO, Sigma-Aldrich) to determine plaque burden. Atherosclerotic plaques located in the aortic root were analyzed by immunohistochemistry at 3 different sections sliced at equally spaced intervals (every 50 μm). The size of the necrotic core was measured on a hematoxylin-eosin (H&E) staining according to a standard method [26]. A 3000 μm^2 minimum threshold was implemented in order to avoid counting of regions that likely do not represent necrotic core areas. The size of the necrotic core was determined by measuring the area of the necrotic core divided by the total plaque size. A Sirius red (Sigma-Aldrich) staining was used for detection of total collagen. Collagen type I was detected on Sirius red-stained sections visualized under polarized light [27]. Apoptosis was determined by anti-cleaved caspase-3 (9661, Cell signaling Technology) and TUNEL (S7101, Millipore) staining. Plaques were further analyzed by immunohistochemistry with the following primary antibodies: mouse anti-α-SMC-actin (A2547, Sigma-Aldrich) and rabbit anti-MMP13 (ab39012, Abcam). The minimum thickness of the fibrous cap within each plaque was measured on an α-SMC-actin staining. Frozen sections of the plaques were analyzed with rabbit anti-Moma2 (MCA519, Serotec), rabbit anti-8-oxodG (orb10011, Biorbyt) and rabbit anti-iNOS (BML-SA200, Enzo Life Sciences). Isotype IgG controls were used as negative controls to assess non-specific background signals of the primary antibodies. Thereafter, tissue sections were incubated with species-appropriate HRP-conjugated secondary antibodies followed by 60 min of reactive ABC. 3,3'-diaminobenzidine or 3-amino-9-ethylcarbazole were used as a chromogen. All images were acquired with Universal Grab 6.1 software using an Olympus BX40 microscope and quantified with Image J software.

2.3. Cell culture

Bone marrow-derived macrophages (BMDM) were harvested by flushing bone marrow from the hind limbs of mice. Cells were cultured for 7 d in RPMI medium (Gibco Life Technologies) supplemented with 15% L-cell conditioned medium (LCCM) containing monocyte colony stimulating factor (M-CSF). To polarize BMDM into M1 macrophages, cells were incubated for 24 h with 100 ng/ml LPS (Sigma-Aldrich). To induce oxidative stress-mediated necrosis, BMDM were treated with 0.5 mol/l and 1 mmol/l *tert*-butyl hydroperoxide (tBHP, Sigma Aldrich) for 2 h and 4 h. Intracellular and mitochondrial ROS was measured using the fluorogenic marker 2′,7′-dichlorofluorescin diacetate (DCFDA, Molecular Probes) and MitoSOX Red (Molecular Probes), respectively. After incubation

with 25 μmol/l carboxy-H_2DCFDA for 1 h or 5 μmol/l MitoSOX for 30 min in HBSS (Gibco Life Technologies), cells were collected and centrifuged. Cell pellet is then resuspended in FACS-buffer (PBS containing 0.1% BSA and 0.05% sodium azide) and analyzed with BD Accuri flow cytometer. Necrosis was monitored by propidium iodide (PI) labeling. Briefly, cells were labeled with 1 μg/ml PI (Molecular Probes) and 5 μg/ml Hoechst 33342 (Life Technologies) and immediately visualized by fluorescence microscopy (EVOS® FL Cell Imaging System). The percentage of PI-positive cells is a measure for the degree of necrosis. To induce apoptosis and necroptosis, BMDM were treated for 24 h with 30 μg/ml cycloheximide (Sigma-Aldrich) or 100 ng/ml LPS and 20 μmol/l zVAD-fmk (Enzo Life Sciences), respectively. Necrostatin-1 (Enzo Life Sciences) was used as RIPK1 inhibitor.

2.4. Western blotting

Cells were lysed in Laemmli sample buffer (Bio-rad) containing β-mercaptoethanol (Sigma-Aldrich) and boiled for 4 min. Tissues samples were first homogenized in RIPA buffer (Sigma-Aldrich) and protein content was determined using BCA method (Thermo Scientific) before mixing with Laemmli sample buffer. Samples were loaded on Bolt 4–12% Bis-Tris gels (Life Technologies) and after electrophoresis transferred to Immobilon-P membranes (Millipore). Membranes were probed with rabbit anti-cleaved caspase-3 (9661, Cell signaling Technologies), rabbit anti-P-NF-κB (3031, Cell signaling Technologies), rabbit anti-total NF-κB (3034, Cell signaling Technologies), hamster anti-TNFα (1221-00, Genzyme) or mouse anti-β-actin (A5441, clone AC-15, Sigma-Aldrich) primary antibodies. Subsequently, membranes were incubated with HRP-conjugated secondary antibodies (Dako) to allow chemiluminescent detection. In some experiments, supernatant was collected and the extracellular proteins were precipitated with 10% trichloroacetic acid (Sigma-Aldrich). After incubation on ice for 15 min, supernatant was centrifuged for 10 min at 2500 g. The protein pellet was resuspended in Laemmli sample buffer containing β-mercaptoethanol. The release of HMGB1 in supernatant during necrosis was detected via western blotting using rabbit anti-HMGB1 (ab18256, Abcam) antibody.

2.5. Real time RT-PCR

Total RNA was prepared using the Nucleospin RNA Kit (Filter Service). Cell culture samples were analyzed for *iNOS* using a TaqMan gene expression assay (Mm00440502_m1, Applied Biosystems). *β-actin* (Mm00607939_s1) was used as reference gene. Tissue samples were analyzed for *TNFα*, *IL6*, *IL1β*, *iNOS*, *HMGB1*, *RAGE* and *TLR4* expression using SYBR Green (GC Biotech). The gene-specific primers (Sigma-Aldrich) are listed in Table S1. Real time RT-PCR was performed on an ABI Prism 7300 sequence detector system (Applied Biosystems). The parameters for PCR amplification were 95 °C for 10 min followed by 40 cycles of 95 °C for 15 s and 60 °C for 1 min. In case of SYBR Green analysis, an additional step of 72 °C for 30 s and a dissociation stage were added. Relative expression of mRNA was calculated using qBASE + software (Biogazelle) [28].

2.6. Statistical analysis

All data were analyzed with SPSS 22.0 software (SPSS Inc.) and presented as mean ± SEM. Statistical tests are mentioned in the figure legends. Differences were considered significant at $p < 0.05$.

3. Results

3.1. NecroX-7 reduces total aortic plaque burden in *Apoe*$^{-/-}$ mice without affecting total plasma cholesterol levels

Apoe$^{-/-}$ mice were treated with NecroX-7 (30 mg/kg body weight) or vehicle 3 times per week and fed a western-type diet for 16 weeks to induce atherosclerotic plaque formation. Oil Red O staining of the thoracic aorta showed a significant decrease in atherosclerotic plaque formation, particularly in the aortic arch of NecroX-7-treated mice as compared to vehicle-treated control mice (Fig. S1A). Body weight, total cholesterol, LDL cholesterol and triglyceride plasma levels were not significantly altered in NecroX-7-treated mice as compared to controls (Table 1). Moreover, NecroX-7 treatment did not affect [oxLDL]/[LDL] and malondialdehyde plasma levels (Table 1), indicating that NecroX-7 does not inhibit oxidation of LDL and lipid peroxidation in WD-fed *Apoe*$^{-/-}$ mice.

3.2. NecroX-7 increases features of atherosclerotic plaque stability in *Apoe*$^{-/-}$ mice

To evaluate the effect of NecroX-7 on plaque size and composition, atherosclerotic plaques located in the aortic root were analyzed. NecroX-7 treatment significantly reduced the necrotic core area as illustrated by smaller and less abundant necrotic cores (Fig. 1A), but did not affect plaque apoptosis (Fig. 1B and Table 1). However, neither plaque size nor macrophage content was altered between both groups (Table 1). Because a reduction in the necrotic core area is a key event in plaque stabilization, other features of plaque stability were examined. Total collagen, in particular collagen type I, was significantly increased in plaques of NecroX-7-treated versus vehicle-treated mice (Fig. 2A and B). Moreover, smooth muscle cell content and minimum fibrous cap thickness were significantly elevated in plaques of NecroX-7-treated mice (Table 1 and Fig. 2C). Interestingly, MMP13 expression, also known as collagenase 3, was significantly decreased in plaques of NecroX-7-treated mice (Fig. 2D). Further analysis showed that there was a significant correlation between the amount of collagen and the number of smooth muscle cells ($p = 0.025$) as well as an inverse association between collagen amount and MMP13 expression in the plaque ($p = 0.015$) (Fig. S1B). These data suggest that the increase in collagen content in plaques of NecroX-7-treated *Apoe*$^{-/-}$ mice is likely due to a combination of increased smooth muscle cell content and decreased MMP13-mediated degradation.

Table 1
Characteristics of vehicle-treated and NecroX-7-treated *Apoe*$^{-/-}$ mice after 16 weeks on western-type diet

	Vehicle	NecroX-7
General		
Body weight (g)[b]	34 ± 1	33 ± 1
Total cholesterol[a,b]	482 ± 25	465 ± 28
LDL cholesterol[a,b]	349 ± 19	315 ± 17
Triglycerides[a,b]	154 ± 13	122 ± 21
[oxLDL]/[LDL][a,b]	0.12 ± 0.01	0.11 ± 0.01
MDA (μmol/l)[b]	0.71 ± 0.05	0.62 ± 0.05
Aortic root plaque		
Plaque area (x10^3 μm^2)[c]	176 ± 6	168 ± 5
# TUNEL positive cells/mm^2 plaque area[c]	46 ± 10	52 ± 7
Moma-2 positive area (%)[c]	1.2 ± 0.1	1.4 ± 0.1
α-SMC-actin positive area (%)[c]	2.5 ± 0.2	3.2 ± 0.2*

*$p < 0.05$ *vs.* vehicle.
[a] mg/dl.
[b] Student *t*-test.
[c] Repeated measure.

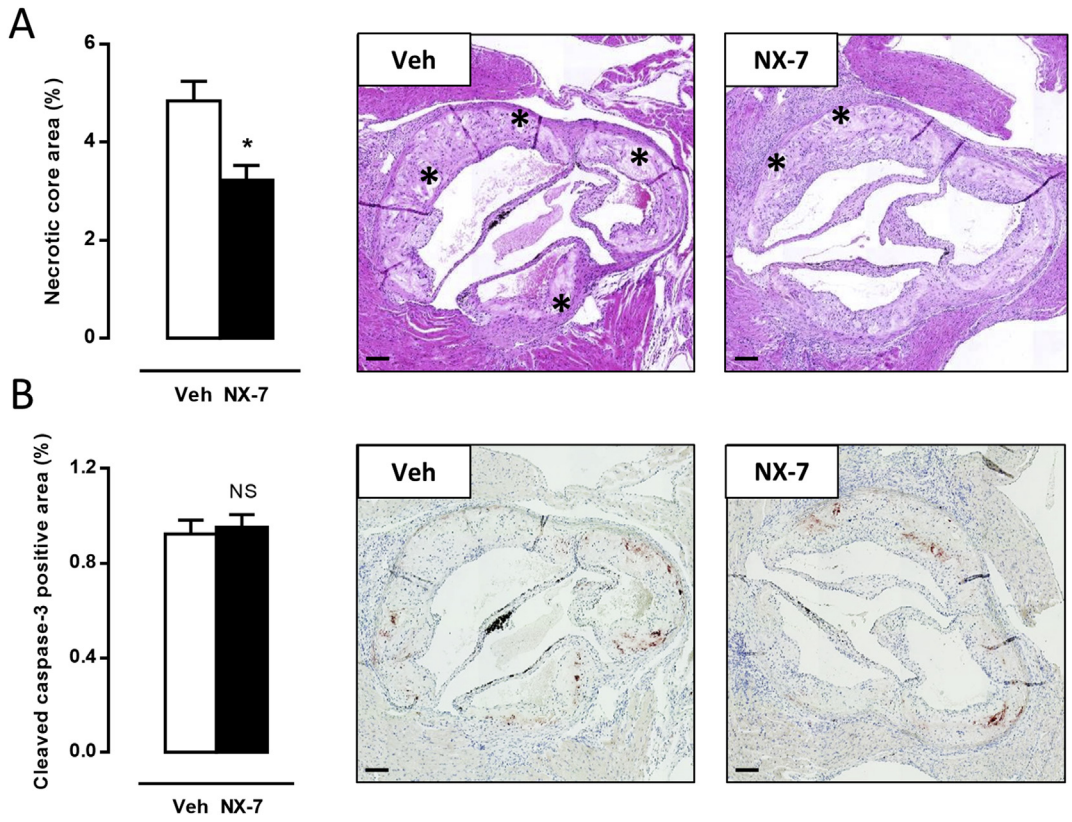

Fig. 1. NecroX-7 reduces necrotic core formation in atherosclerotic plaques of *Apoe*$^{-/-}$ mice. (A) Sections of the aortic root of vehicle-treated (Veh) and NecroX-7-treated (NX-7) *Apoe*$^{-/-}$ mice were stained with hematoxylin-eosin to quantify the necrotic core area (*$p < 0.05$ *vs.* vehicle; n = 25; repeated measure). Necrotic cores are indicated by an asterisk. (B) Serial sections were immunostained for cleaved caspase-3 to measure the percentage of apoptosis (NS, not significant *vs.* vehicle; n = 25; repeated measure). Scale bars: 100 μm.

3.3. NecroX-7 reduces atherosclerotic plaque oxidative stress and inflammation

According to an immunohistochemical staining of 8-oxodG, a well-known marker of oxidative stress-induced DNA damage, 4 out of 11 control plaques showed signs of oxidative stress while none of the plaques of NecroX-7-treated mice stained positive for 8-oxodG (Fig. 3A). In control mice, 8-oxodG-positivity was mostly observed in the proximity of the necrotic core and revealed both nuclear and non-nuclear oxidative DNA damage. Also iNOS expression was significantly decreased in plaques of NecroX-7-treated mice, suggestive of reduced oxidative stress and inflammation (Fig. 3B). Real time RT-PCR analysis of whole plaque lysates of NecroX-7-treated mice revealed a significant decrease of multiple inflammation markers including *TNFα*, *IL1β*, *iNOS*, high mobility group box 1 *(HMGB1)* and receptor for advanced glycation end products *(RAGE)* as compared to vehicle-treated mice (Fig. 3C). There was also a trend ($p = 0.06$) for reduced *IL6* mRNA expression in NecroX-7-treated plaques. Moreover, the reduced expression of inflammation markers in NecroX-7-treated plaques was associated with hypophosphorylation of NF-κB (Fig. 3D). Of note, the use of whole plaque lysates did not allow us to identify the cell-type specific sources of the different inflammatory mediators.

3.4. NecroX-7 inhibits oxidative stress-induced necrosis in macrophages

To validate the antioxidative properties of NecroX-7, oxidative stress was induced in bone marrow-derived macrophages (BMDM) with *tert*-butyl hydroperoxide (tBHP). High doses of tBHP (0.5 and 1 mmol/l) generated high levels of intracellular and mitochondrial ROS after 2 h and 4 h treatment in a dose-dependent manner as shown by DCFDA and MitoSOX labeling, respectively (Fig. 4A and B). NecroX-7 strongly decreased intracellular ROS as well as mitochondrial ROS levels in all conditions (Fig. 4A and B). Moreover, NecroX-7 inhibited iNOS expression in M1-polarized BMDM exposed to tBHP (Fig. 4C), an indirect measure for reduced oxidative stress.

To link the antioxidative effects of NecroX-7 with its cytoprotective and anti-necrotic potential, the viability of tBHP-treated BMDM was assessed by multiple techniques. According to morphological analysis, NecroX-7 improved cell viability of tBHP-treated BMDM substantially (Fig. 4D). In particular, the incidence of cell oncosis was decreased by about 90% after NecroX-7 treatment. Moreover, NecroX-7 diminished HMGB1 release in the supernatant of tBHP-treated BMDM (Fig. 4E) and preserved cell membrane integrity as shown by reduced PI labeling (Fig. 4F). These data indicate that NecroX-7 inhibits necrosis in BMDM in the presence of a powerful oxidant. Importantly, doses of 0.5 and 1 mmol/l tBHP used in these experiments induced neither apoptosis (Fig. S2A and S2B) nor RIPK1/RIPK3-dependent necroptosis (Fig. S3), indicating that high doses of tBHP were a suitable inductor of oxidative stress-induced necrosis in BMDM.

3.5. NecroX-7 inhibits neither LPS-induced necroptosis nor cycloheximide-induced apoptosis

To investigate whether NecroX-7 inhibits necroptosis, BMDM were treated with LPS (100 ng/ml) and zVAD-fmk (20 μmol/l) for 24 h. Necroptosis was induced in wild-type BMDM but not in

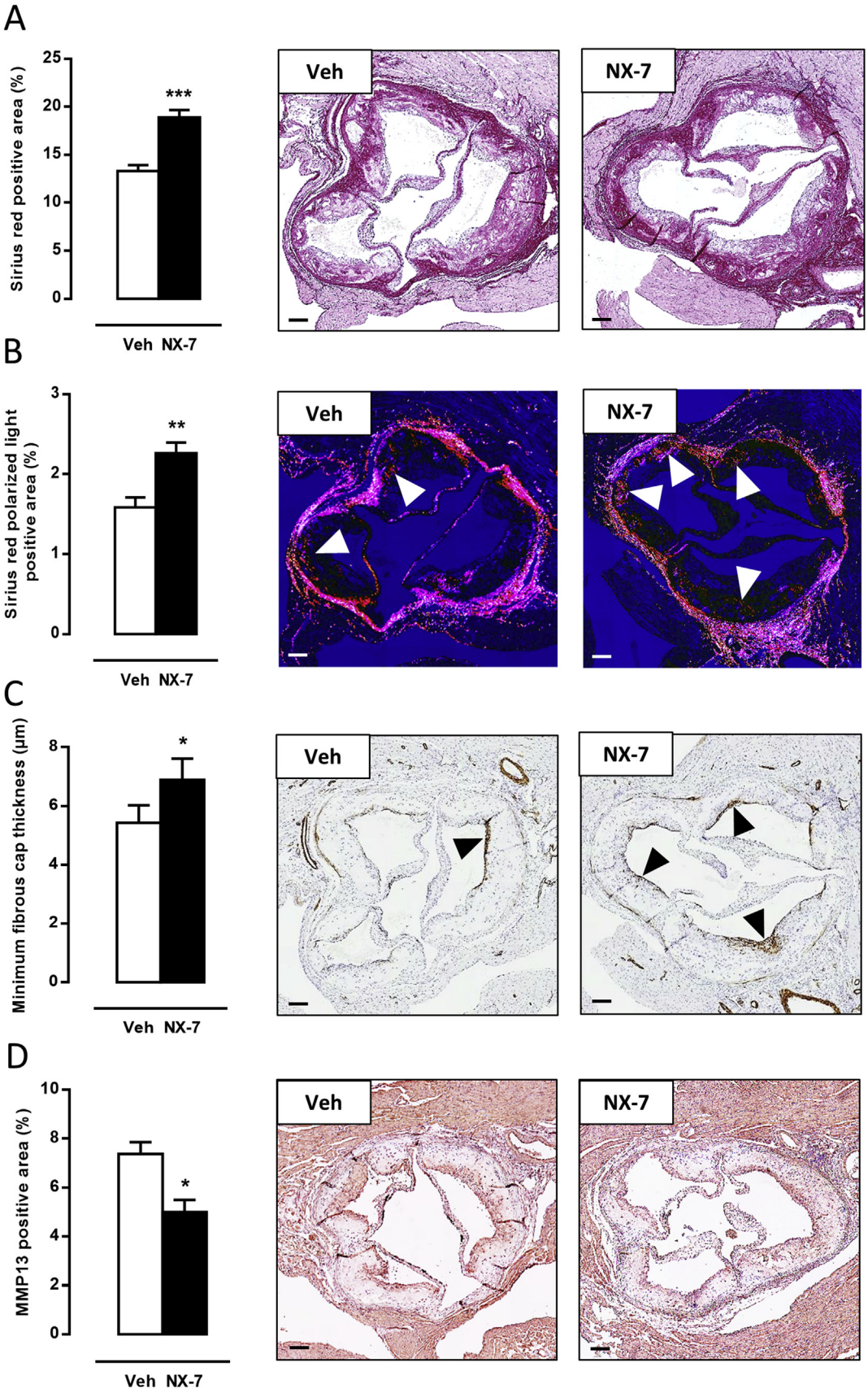

Fig. 2. NecroX-7 increases collagen deposition and formation of a thick fibrous cap in atherosclerotic plaques of *Apoe*$^{-/-}$ mice. (A, B) Sections of the aortic root of vehicle-treated (Veh) and NecroX-7-treated (NX-7) *Apoe*$^{-/-}$ mice were stained with Sirius red to quantify total collagen (A) and collagen type I visualized under polarized light (B) (red, indicated by white arrowheads) (***$p < 0.001$, **$p < 0.01$, *vs.* vehicle; n = 25; repeated measure). (C) Serial sections were immunostained for α-SMC-actin to measure the minimum fibrous cap thickness (indicated by black arrowheads) (*$p < 0.05$ *vs.* vehicle; n = 8 measurements/mouse; univariate). (D) Serial sections were immunostained for MMP13 (*$p < 0.05$ *vs.* vehicle; n = 10; repeated measure). Scale bars: 100 µm.

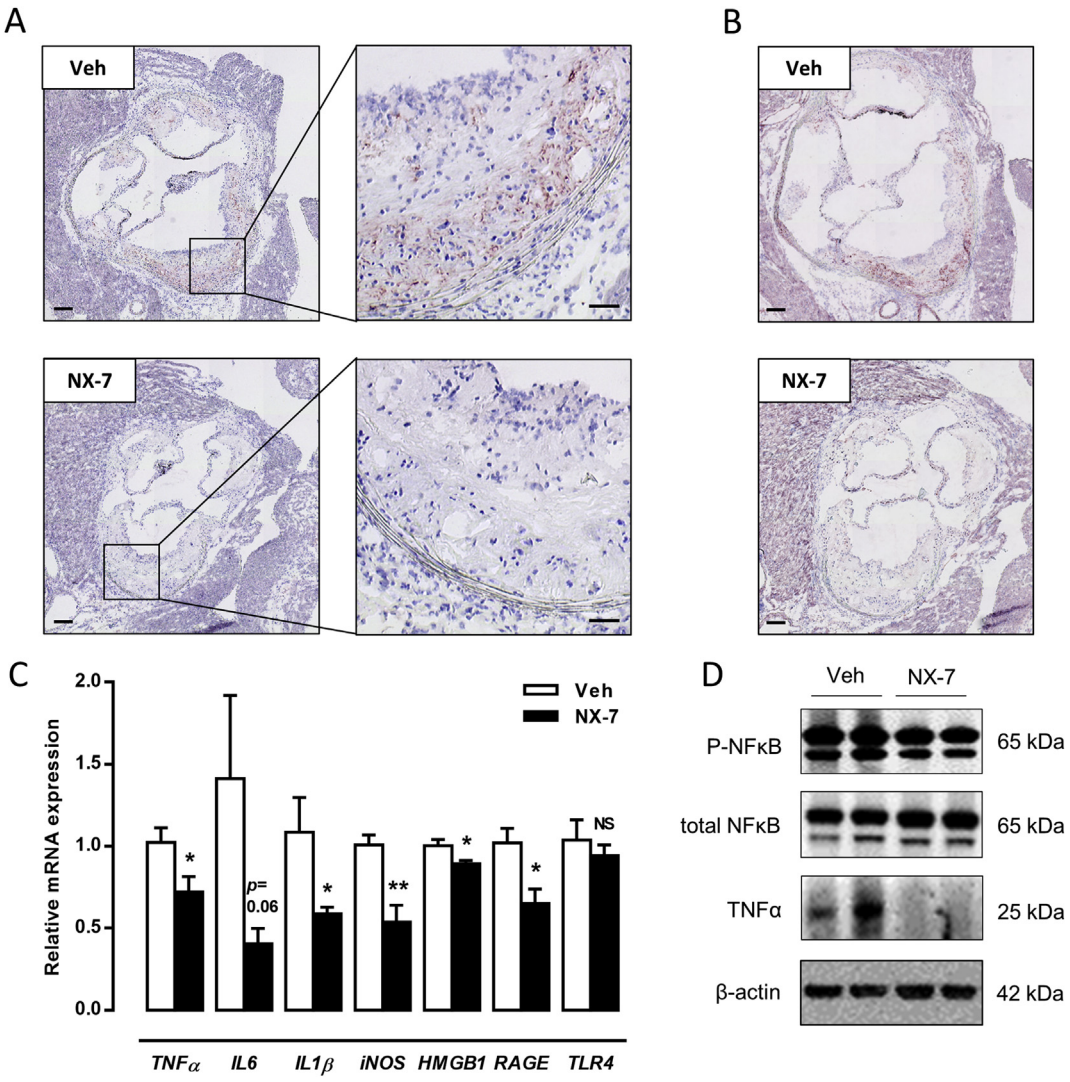

Fig. 3. NecroX-7 reduces oxidative stress and inflammation in atherosclerotic plaques of *Apoe*$^{-/-}$ mice. (A) Sections of the aortic root of vehicle-treated (Veh) and NecroX-7-treated (NX-7) *Apoe*$^{-/-}$ mice were immunostained for 8-oxodG to detect oxidative stress ($p < 0.05$; Chi square, 4/11 (Veh) *vs*. 0/9 (NX-7)). Scale bars: 150 μm and 25 μm (detail). (B) Serial sections were immunostained for iNOS. Scale bar: 150 μm. (C) Real time RT-PCR analysis on whole plaque lysates for *TNFα*, *IL6*, *IL1β*, *iNOS*, *HMGB1*, *RAGE* and *TLR4* mRNA expression. ($^{*}p < 0.05$, $^{**}p < 0.01$; NS, not significant *vs*. vehicle; n = 6 aortas/group; Student *t*-test). (D) Western blot analysis on plaque lysates for P-NF-κB, total NF-κB and TNFα. β-actin was used as loading control. n = 2 pooled samples/group. Each pooled sample consists of atherosclerotic tissue from 3 different mice due to low protein amount.

Necrostatin-1 (Nec-1, RIPK1 inhibitor) treated or *Ripk3*$^{-/-}$ BMDM. However, NecroX-7 treatment did not affect LPS + zVAD-fmk-induced necroptosis (Fig. S4A).

To study whether NecroX-7 targets apoptosis, BMDM were treated with the protein synthesis inhibitor cycloheximide (30 μg/ml) for 24 h. According to immunocytochemistry and western blot analysis of cleaved caspase-3, NecroX-7 did not inhibit cycloheximide-induced macrophage apoptosis (Fig. S4B and S4C).

4. Discussion

Recently, NecroX compounds have been successfully tested in several pathologies including oxidative stress-induced cardiomyopathy, hepatic and renal ischemia-reperfusion injury, nonalcoholic steatohepatitis, allergic lung inflammation and acute graft-versus-host-disease [20–22,29–35]. As a result, NecroX-7 is currently being tested in ST-segment elevated myocardial infarction (STEMI) patients before percutaneous coronary intervention to reduce myocardial infarct size (https://clinicaltrials.gov, identifier NCT02070471). In the present study, we tested the potential plaque stabilizing effects of NecroX-7 in *Apoe*$^{-/-}$ mice, a model of atherosclerosis.

From a general point of view, unstable plaques are characterized by a highly inflammatory cell content, a large necrotic core and a thin fibrous cap consisting of a low amount of smooth muscle cells and extracellular matrix (e.g. collagen) [36]. NecroX-7 was able to improve plaque stability at different levels. Firstly, NecroX-7 reduced necrotic core area, albeit this effect did not result in smaller plaques. Secondly, we observed an increase in total collagen content and minimum fibrous cap thickness. A correlation analysis showed that the increase in total collagen content is most likely due to an increase in collagen deposition (owing to increased smooth muscle cell amount) and a decrease in MMP13-mediated collagen degradation. Though, to fully strengthen the latter view, measurement of MMP13 collagenolytic activity is required. Thirdly, even though the amount of macrophages was not different after NecroX-7 treatment, plaques developed a less inflammatory phenotype. Multiple inflammation markers such as *TNFα*, *IL1β*, *iNOS*, *HMGB1*

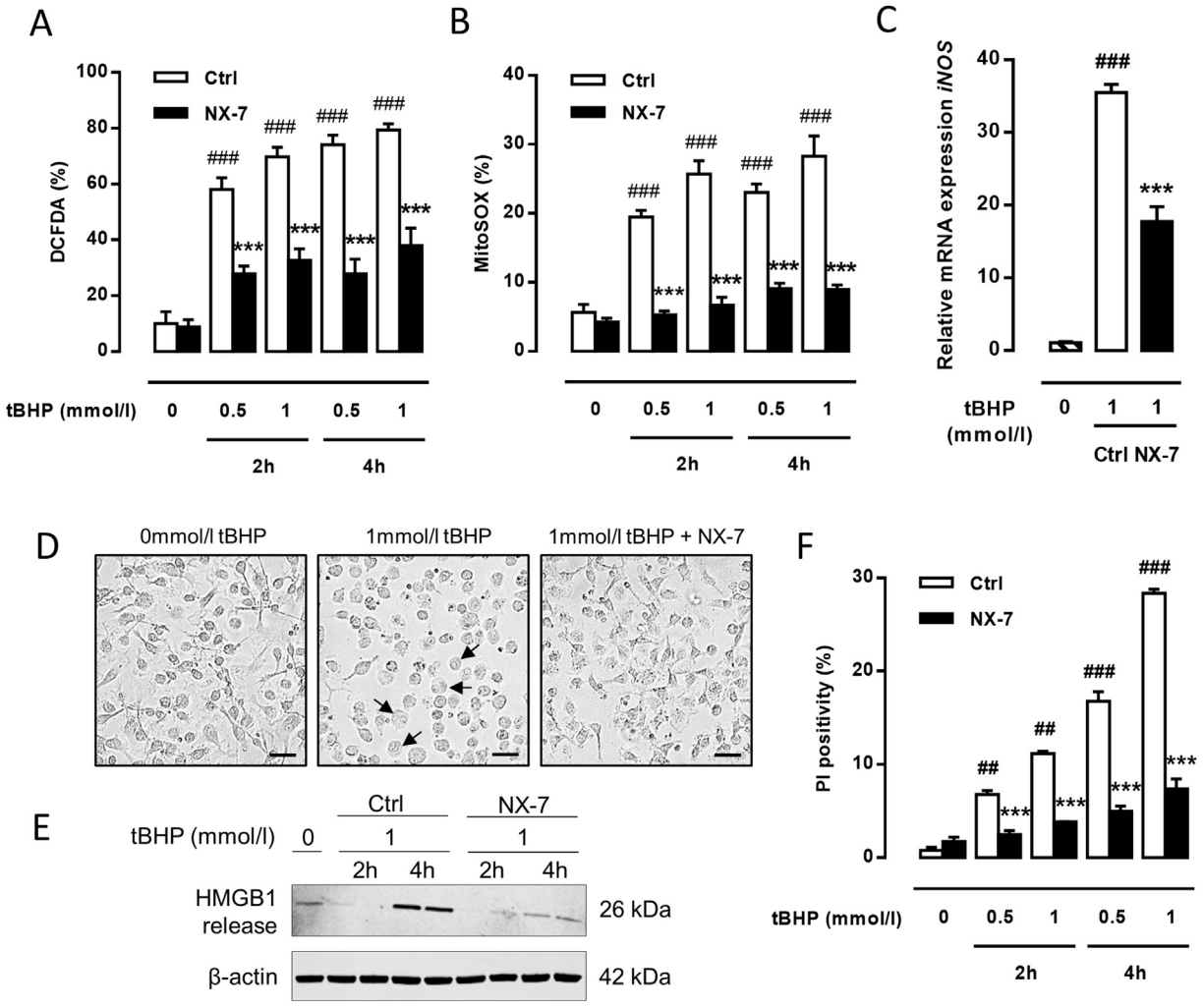

Fig. 4. NecroX-7 inhibits oxidative stress-induced necrosis in macrophages. (A,B) Bone marrow-derived macrophages (BMDM) were exposed to 0 mmol/l, 0.5 mmol/l or 1 mmol/l tBHP for 2 h or 4 h and treated with 10 μmol/l NecroX-7 (NX-7) or left untreated (Ctrl). Intracellular and mitochondrial ROS generation was monitored by DCFDA and MitoSOX labeling, respectively. ($^{***}p < 0.001$ *vs.* Ctrl; $^{###}p < 0.001$ *vs.* 0 mmol/l; n = 2 experiments in duplicate; factorial ANOVA). (C) BMDM were polarized to M1 macrophages, exposed to 0 mmol/l or 1 mmol/l tBHP for 4 h in the presence (NX-7) or absence (Ctrl) of 10 μmol/l NecroX-7. *iNOS* expression was analyzed by real time RT-PCR ($^{***}p < 0.001$ *vs.* Ctrl; $^{###}p < 0.001$ *vs.* 0 mmol/l; n = 2 independent experiments in tetraplicate; one way ANOVA with Bonferroni *post hoc* test). (D) Representative images of BMDM exposed to 0 mmol/l tBHP (left panel), 1 mmol/l tBHP (middle panel), or 1 mmol/l tBHP in combination with 10 μmol/l NecroX-7 (right panel) for 4 h. Necrotic BMDM (indicated by black arrows) were characterized by an increase in cell volume (oncosis) and a translucent cytoplasm. Scale bar: 25 μm. (E) BMDM were exposed to 0 mmol/l or 1 mmol/l tBHP for 2 h or 4 h and treated with 10 μmol/l NecroX-7 (NX-7) or left untreated (Ctrl). Necrosis was determined by western blot analysis of HMGB1 release in supernatant. Corresponding cell lysates were analyzed for β-actin as internal control. Bands are shown in duplicate. (F) BMDM were exposed to 0 mmol/l, 0.5 mmol/l or 1 mmol/l tBHP for 2 h or 4 h and treated with 10 μmol/l NecroX-7 (NX-7) or left untreated (Ctrl). Necrosis was determined by PI labeling ($^{***}p < 0.001$ *vs.* Ctrl; $^{###}p < 0.001$ *vs.* 0 mmol/l; n = 2 experiments with 2 counting regions of 300 cells/region in duplicate; factorial ANOVA).

and *RAGE* were decreased in plaques of NecroX-7-treated *Apoe*$^{-/-}$ mice, which was associated with reduced NF-κB activation. Of all pro-inflammatory mediators, HMGB1 is one of the most studied molecules associated with necrosis. HMGB1 is a nuclear protein that is passively released from necrotic or damaged cells, but not during apoptosis and secondary necrosis [37]. Once released, HMGB1 acts as a danger-associated molecular pattern (DAMP) signal and stimulates macrophages to produce pro-inflammatory cytokines such as TNFα, IL6 and IL1β via activation of NF-κB and MAPK signaling pathways upon binding with the receptor for advanced glycation end products (RAGE) or members of the toll-like receptor family (e.g. TLR4) [38–40]. On the other hand, pro-inflammatory cytokines may stimulate *HMGB1* mRNA expression in macrophages and promote the release of HMGB1 in an active manner [40,41]. Our data indicate that NecroX-7 downregulates the HMGB1/RAGE axis and attenuates inflammation in a NF-κB-dependent manner in atherosclerotic plaques of WD-fed *Apoe*$^{-/-}$ mice.

Our *in vitro* experiments demonstrated that NecroX-7 inhibits oxidative stress-induced necrosis in primary macrophages, but targets neither LPS-induced necroptosis nor cycloheximide-induced apoptosis. NecroX-7 inhibits necrosis in tBHP-treated BMDM by preventing HMGB1 release and preserving cell membrane integrity as shown by reduced PI labeling. Moreover, NecroX-7 inhibits the generation of mitochondrial ROS (mtROS) in tBHP-treated BMDM. The antioxidative action of NecroX-7 may account, at least partially, for its anti-necrotic potential. Indeed, the imbalance between mtROS production and mtROS elimination may lead to excessive mtROS levels and subsequent cell death [42]. According to various reports, excessive mtROS promotes the progression of atherosclerosis in both patients and mouse models [14–18]. In the present study, NecroX-7 lowered oxidative stress in

atherosclerotic plaques of *Apoe*$^{-/-}$ mice as detected by 8-oxodG. This structure is a typical oxidative modification of nuclear DNA and mtDNA [43], and a recently accepted marker of mtROS in murine atherosclerotic lesions [17].

Although the detrimental role of oxidative stress in atherosclerosis is broadly accepted, the results of clinical trials investigating antioxidative compounds (e.g. vitamin E) are rather disappointing (reviewed in Refs. [44,45]). Possibly, these compounds convert into pro-oxidants when scavenging ROS and/or impair mitochondrial function [46]. Moreover, these classical antioxidants are widely distributed throughout the body and block several oxidative reactions (e.g. propagation of lipid peroxidation) though they do not target mitochondrial oxidative damage directly [47]. Mitochondria-targeted antioxidants such as NecroX-7 are chemically designed in such a way that they selectively concentrate within the mitochondria in the tissue [47]. In this way, these antioxidants accumulate in high amounts at the site where most ROS are generated. The unique chemical moiety of 7-amino (indole) allows NecroX-7 to preferentially accumulate in the mitochondria and thus to inhibit the generation of mtROS, mitochondrial depolarization, ATP depletion and subsequent necrosis. Additional evidence shows that NecroX-7 inhibits necrosis and preserves mitochondrial membrane potential much more effectively than the classical antioxidants, presumably by inhibition of the opening of the mitochondrial permeability transmission pore (mPTP) [23]. Moreover, NecroX-7 significantly inhibits myocardial necrosis after ischemia-reperfusion injury in rats as compared to controls and cyclosporine A, a well-known mPTP blocker [23]. To our knowledge, these anti-necrotic effects have not been described for other currently available antioxidative compounds in atherosclerosis studies. In addition, NecroX-7 was not able to lower [oxLDL]/[LDL] and malondialdehyde levels in plasma of WD-fed *Apoe*$^{-/-}$ mice, indicating that inhibition of lipid (per)oxidation reactions is not its main mode of action to reduce atherogenesis, in contrast to the classical antioxidants such as vitamin E [48]. Although we cannot exclude that the decrease in plaque inflammation in NecroX-7-treated mice is a result of reduced mtROS, above-mentioned data indicate that NecroX-7 exhibits discernible anti-necrotic effects which are likely accountable for the decreased inflammation. Furthermore, it is worthwhile to mention that comparable plaque stabilizing effects were observed in *Apoe*$^{-/-}$ mice treated with MitoQ, one of the few antioxidants that selectively target the mitochondria. MitoQ does not affect total plaque size, smooth muscle content and apoptosis, but reduces the number of plaque macrophages [49]. Unfortunately, the effect of MitoQ on necrotic core formation was not examined.

Our study demonstrates that inhibition of important triggers of necrosis such as mitochondrial oxidative stress during atherogenesis attenuates the severity of the disease. However, from a translational point of view, more experiments evaluating the effect of NecroX-7 on established plaques would be extremely valuable. With regard to its suitability in humans, NecroX-7 is now being tested in phase II clinical trials to evaluate its efficacy, safety and pharmacokinetic properties (https://clinicaltrials.gov, identifier NCT02070471). Moreover, analysis of the cytokine profiles of healthy subjects showed that NecroX-7 does not induce a pathological inflammatory response, at least not after one single injection [33]. Because the treatment of atherosclerosis requires a chronic approach, the evaluation of the safety of NecroX-7 during chronic administration should be included in future trials.

In conclusion, NecroX-7 improves features of atherosclerotic plaque stability in 16 week western-type diet-fed *Apoe*$^{-/-}$ mice by reducing necrotic core formation, oxidative stress and inflammation, and by increasing collagen deposition and fibrous cap thickness. Given the multifaceted pathophysiology of atherosclerosis and the pleiotropic efficacy of NecroX-7, this compound could be a new attractive therapeutic drug in the treatment of atherosclerosis.

Conflict of interest

The authors declared they do not have anything to disclose regarding conflict of interest with respect to this manuscript.

Financial support

This work was supported by the Fund for Scientific Research (FWO)-Flanders (project N° G.0074.12N) and the University of Antwerp (TOP-BOF29068). Research in the Vandenabeele unit is supported by Belgian grants (Interuniversity Attraction Poles, IAP 7/32), Flemish grants (Research Foundation Flanders) – G.0875.11, G.0973.11, G.0A45.12N, G.0787.13N, G.0172.12N, Methusalem grant (BOF09/01M00709). Mandy O.J. Grootaert is a fellow of the Agency for Innovation by Science and Technology (IWT).

Acknowledgements

The authors thank Rita Van den Bossche, Hermine Fret, Anne-Elise Van Hoydonck, Cor Van Hove and Caroline Verstraete for excellent technical support. The authors acknowledge the Center for Oncological Research (CORE) at the University of Antwerp under the supervision of Prof. dr. Filip Lardon for the use of the EVOS® FL Cell Imaging System. The authors also thank Dr. Wilhelmus Kwanten and Prof. dr. Paul Cos for fruitful discussions.

Appendix A. Supplementary data

Supplementary data related to this article can be found at http://dx.doi.org/10.1016/j.atherosclerosis.2016.06.045.

References

[1] P.W. Fok, Growth of necrotic cores in atherosclerotic plaque, Math. Med. Biol. 29 (2012) 301–327.
[2] R. Virmani, A.P. Burke, J. Willerson, A. Farb, J. Narula, F.D. Kolodgie, The pathology of vulnerable plaque, in: R. Virmani, J. Narula, M. Leon, J. Willerson (Eds.), The Vulnerable Atherosclerotic Plaque: Strategies for Diagnosis and Management, Blackwell Futura, Malden, 2007, pp. 21–36.
[3] I. Tabas, Consequences and therapeutic implications of macrophage apoptosis in atherosclerosis: the importance of lesion stage and phagocytic efficiency, Arterioscler. Thromb. Vasc. Biol. 25 (2005) 2255–2264.
[4] G. Majno, I. Joris, Apoptosis, oncosis, and necrosis. An overview of cell death, Am. J. Pathol. 146 (1995) 3–15.
[5] T. Seimon, I. Tabas, Mechanisms and consequences of macrophage apoptosis in atherosclerosis, J. Lipid Res. (2009) 50. Suppl:S382-S387.
[6] W. Martinet, D.M. Schrijvers, G.R.Y. De Meyer, Necrotic cell death in atherosclerosis, Basic Res. Cardiol. 106 (2011) 749–760.
[7] D.M. Schrijvers, G.R.Y. De Meyer, A.G. Herman, W. Martinet, Phagocytosis in atherosclerosis: molecular mechanisms and implications for plaque progression and stability, Cardiovasc Res. 73 (2007) 470–480.
[8] R.Y. Ball, E.C. Stowers, J.H. Burton, N.R. Cary, J.N. Skepper, M.J. Mitchinson, Evidence that the death of macrophage foam cells contributes to the lipid core of atheroma, Atherosclerosis 114 (1995) 45–54.
[9] M. Crisby, B. Kallin, J. Thyberg, B. Zhivotovsky, S. Orrenius, V. Kostulas, J. Nilsson, Cell death in human atherosclerotic plaques involves both oncosis and apoptosis, Atherosclerosis 130 (1997) 17–27.
[10] W. Declercq, T. Vanden Berghe, P. Vandenabeele, RIP kinases at the crossroads of cell death and survival, Cell 138 (2009) 229–232.
[11] D.W. Zhang, J. Shao, J. Lin, N. Zhang, B.J. Lu, S.C. Lin, M.Q. Dong, J. Han, RIP3, an energy metabolism regulator that switches TNF-induced cell death from apoptosis to necrosis, Science 325 (2009) 332–336.
[12] T. Vanden Berghe, A. Linkermann, S. Jouan-Lanhouet, H. Walczak, P. Vandenabeele, Regulated necrosis: the expanding network of non-apoptotic cell death pathways, Nat. Rev. Mol. Cell Biol. 15 (2014) 135–147.
[13] J. Lin, et al., A role of RIP3-mediated macrophage necrosis in atherosclerosis development, Cell Rep. 3 (2013) 200–210.
[14] C.M. Harrison, M. Pompilius, K.E. Pinkerton, S.W. Ballinger, Mitochondrial oxidative stress significantly influences atherogenic risk and cytokine-induced oxidant production, Environ. Health Perspect. 119 (2011) 676–681.
[15] S.W. Ballinger, et al., Mitochondrial integrity and function in atherogenesis,

Circulation 106 (2002) 544–549.
[16] E. Ari, Y. Kaya, H. Demir, A. Cebi, H.H. Alp, E. Bakan, D. Odabasi, S. Keskin, Oxidative DNA damage correlates with carotid artery atherosclerosis in hemodialysis patients, Hemodial. Int. 15 (2011) 453–459.
[17] Y. Wang, G.Z. Wang, P.S. Rabinovitch, I. Tabas, Macrophage mitochondrial oxidative stress promotes atherosclerosis and nuclear factor-kappaB-mediated inflammation in macrophages, Circ. Res. 114 (2014) 421–433.
[18] I. Tabas, Y. Wang, Emerging roles of mitochondria ROS in atherosclerotic lesions: causation or association? J. Atheroscler. Thromb. 21 (2014) 381–390.
[19] H.J. Kim, et al., NecroX as a novel class of mitochondrial reactive oxygen species and ONOO scavenger, Arch. Pharm. Res. 33 (2010) 1813–1823.
[20] J. Park, et al., NecroX-7 prevents oxidative stress-induced cardiomyopathy by inhibition of NADPH oxidase activity in rats, Toxicol. Appl. Pharmacol. 263 (2012) 1–6.
[21] H.K. Chung, et al., The indole derivative NecroX-7 improves nonalcoholic steatohepatitis in ob/ob mice through suppression of mitochondrial ROS/RNS and inflammation, Liver Int. 35 (2015) 1341–1353.
[22] K.I. Im, N. Kim, J.Y. Lim, Y.S. Nam, E.S. Lee, E.J. Kim, H.J. Kim, S.H. Kim, S.G. Cho, The free radical scavenger NecroX-7 attenuates acute graft-versus-host disease via reciprocal regulation of Th1/Regulatory T cells and inhibition of HMGB1 release, J. Immunol. 194 (2015) 5223–5232.
[23] H.J. Cho, I.C. Hwang, J.Y. Kim, H.S. Lee, J. Lee, J. Park, et al., Therapeutic potential of a novel necrosis inhibitor in myocardial ischemia-reperfusion injury, Circ. Res. 117 (2015) A263 (Abstract).
[24] N. Hermans, P. Cos, D.V. Berghe, A.J. Vlietinck, B.T. de, Method development and validation for monitoring in vivo oxidative stress: evaluation of lipid peroxidation and fat-soluble vitamin status by HPLC in rat plasma, J. Chromatogr. B Anal. Technol. Biomed. Life Sci. 822 (2005) 33–39.
[25] K. Newton, X. Sun, V.M. Dixit, Kinase RIP3 is dispensable for normal NF-kappa Bs, signaling by the B-cell and T-cell receptors, tumor necrosis factor receptor 1, and Toll-like receptors 2 and 4, Mol. Cell Biol. 24 (2004) 1464–1469.
[26] T.A. Seimon, Y. Wang, S. Han, T. Senokuchi, D.M. Schrijvers, G. Kuriakose, A.R. Tall, I.A. Tabas, Macrophage deficiency of p38alpha MAPK promotes apoptosis and plaque necrosis in advanced atherosclerotic lesions in mice, J. Clin. Invest. 119 (2009) 886–898.
[27] L.C. Junqueira, W. Cossermelli, R. Brentani, Differential staining of collagens type I, II and III by Sirius Red and polarization microscopy, Arch. Histol. Jpn. 41 (1978) 267–274.
[28] J. Hellemans, G. Mortier, P.A. De, F. Speleman, J. Vandesompele, qBase relative quantification framework and software for management and automated analysis of real-time quantitative PCR data, Genome Biol. 8 (2007) R19.
[29] V.T. Thu, et al., NecroX-5 prevents hypoxia/reoxygenation injury by inhibiting the mitochondrial calcium uniporter, Cardiovasc Res. 94 (2012) 342–350.
[30] J.M. Choi, K.M. Park, S.H. Kim, D.W. Hwang, S.H. Chon, J.H. Lee, S.Y. Lee, Y.J. Lee, Effect of necrosis modulator necrox-7 on hepatic ischemia-reperfusion injury in beagle dogs, Transpl. Proc. 42 (2010) 3414–3421.
[31] J.H. Park, et al., An indole derivative protects against acetaminophen-induced liver injury by directly binding to N-acetyl-p-benzoquinone imine in mice, Antioxid. Redox Signal 18 (2013) 1713–1722.
[32] S.R. Kim, D.I. Kim, S.H. Kim, H. Lee, K.S. Lee, S.H. Cho, Y.C. Lee, NLRP3 inflammasome activation by mitochondrial ROS in bronchial epithelial cells is required for allergic inflammation, Cell Death Dis. 5 (2014) e1498.
[33] E. Shin, Y.C. Lee, S.R. Kim, S.H. Kim, J. Park, Drug signature-based finding of additional clinical use of LC28-0126 for neutrophilic bronchial asthma, Sci. Rep. 5 (2015) 17784.
[34] X. Li, O. Kwon, D.Y. Kim, Y. Taketomi, M. Murakami, H.W. Chang, NecroX-5 suppresses IgE/Ag-stimulated anaphylaxis and mast cell activation by regulating the SHP-1-Syk signaling module, Allergy 71 (2016) 198–209.
[35] S.A. Jin, et al., Beneficial effects of necrosis modulator, indole derivative NecroX-7, on renal ischemia-reperfusion injury in rats, Transpl. Proc. 48 (2016) 199–204.
[36] E. Falk, M. Nakano, J.F. Bentzon, A.V. Finn, R. Virmani, Update on acute coronary syndromes: the pathologists' view, Eur. Heart J. 34 (2013) 719–728.
[37] P. Scaffidi, T. Misteli, M.E. Bianchi, Release of chromatin protein HMGB1 by necrotic cells triggers inflammation, Nature 418 (2002) 191–195.
[38] U. Andersson, et al., High mobility group 1 protein (HMG-1) stimulates proinflammatory cytokine synthesis in human monocytes, J. Exp. Med. 192 (2000) 565–570.
[39] H.H. Erlandsson, U. Andersson, Mini-review: the nuclear protein HMGB1 as a proinflammatory mediator, Eur. J. Immunol. 34 (2004) 1503–1512.
[40] N. Kalinina, A. Agrotis, Y. Antropova, G. DiVitto, P. Kanellakis, G. Kostolias, O. Ilyinskaya, E. Tararak, A. Bobik, Increased expression of the DNA-binding cytokine HMGB1 in human atherosclerotic lesions: role of activated macrophages and cytokines, Arterioscler. Thromb. Vasc. Biol. 24 (2004) 2320–2325.
[41] S. Gardella, C. Andrei, D. Ferrera, L.V. Lotti, M.R. Torrisi, M.E. Bianchi, A. Rubartelli, The nuclear protein HMGB1 is secreted by monocytes via a non-classical, vesicle-mediated secretory pathway, EMBO Rep. 3 (2002) 995–1001.
[42] X. Li, P. Fang, J. Mai, E.T. Choi, H. Wang, X.F. Yang, Targeting mitochondrial reactive oxygen species as novel therapy for inflammatory diseases and cancers, J. Hematol. Oncol. 6 (2013) 19.
[43] N.C. de Souza-Pinto, L. Eide, B.A. Hogue, T. Thybo, T. Stevnsner, E. Seeberg, A. Klungland, V.A. Bohr, Repair of 8-oxodeoxyguanosine lesions in mitochondrial dna depends on the oxoguanine dna glycosylase (OGG1) gene and 8-oxoguanine accumulates in the mitochondrial dna of OGG1-defective mice, Cancer Res. 61 (2001) 5378–5381.
[44] N.R. Madamanchi, A. Vendrov, M.S. Runge, Oxidative stress and vascular disease, Arterioscler. Thromb. Vasc. Biol. 25 (2005) 29–38.
[45] A. Cherubini, G.B. Vigna, G. Zuliani, C. Ruggiero, U. Senin, R. Fellin, Role of antioxidants in atherosclerosis: epidemiological and clinical update, Curr. Pharm. Des. 11 (2005) 2017–2032.
[46] H. Otani, Site-specific antioxidative therapy for prevention of atherosclerosis and cardiovascular disease, Oxid. Med. Cell Longev. 2013 (2013) 796891.
[47] R.A. Smith, M.P. Murphy, Mitochondria-targeted antioxidants as therapies, Discov. Med. 11 (2011) 106–114.
[48] J.M. Upston, L. Kritharides, R. Stocker, The role of vitamin E in atherosclerosis, Prog. Lipid Res. 42 (2003) 405–422.
[49] J.R. Mercer, et al., The mitochondria-targeted antioxidant MitoQ decreases features of the metabolic syndrome in $ATM^{+/-}$/$ApoE^{-/-}$ mice, Free Radic. Biol. Med. 52 (2012) 841–849.